Journal of Molecular Catalysis B: Enzymatic 56 (2009) 215–220

Contents lists available at ScienceDirect

Journal of Molecular Catalysis B: Enzymatic

journal homepage: www.elsevier.com/locate/molcatb

Amperometric hydrogen peroxide biosensor based on the immobilization of HRP on DNA–silver nanohybrids and PDDA-protected gold nanoparticles

Liping Ma, Ruo Yuan*, Yaqin Chai, Shihong Chen

Chongqing Key Laboratory of Analytical Chemistry, College of Chemistry and Chemical Engineering, Southwest University, Chongqing 400715, China

ARTICLE INFO

Article history:
Received 25 January 2008
Received in revised form 2 April 2008
Accepted 4 May 2008
Available online 14 May 2008

Keywords:
DNA–silver nanohybrids
PDDA-protected gold nanoparticles
Hydrogen peroxide biosensor
HRP

ABSTRACT

A novel amperometric hydrogen peroxide biosensor based on the immobilization of horseradish peroxidase (HRP) on DNA–silver nanohybrids (DNA–Ag) and poly(diallyldimethylammonium chloride) (PDDA)-protected gold nanoparticles (PDDA–Au) was successfully fabricated by combining the self-assembly technique with an in situ electrochemical reduction of the DNA–Ag^+ complex. The preparation process of modified electrode was characterized with UV–vis absorption spectroscopy, transmission electron microscopy (TEM) and atomic force microscope (AFM). The electrochemical characteristics of the biosensor were studied by cyclic voltammetry and chronoamperometry. Experimental conditions influencing the biosensor performance such as pH, potential were optimized. The resulting biosensor (HRP/DNA–Ag/PDDA–Au/DNA–Ag/Au electrode) showed a linear response to H_2O_2 over a concentration range from 7.0 μM to 7.8 mM with a detection limit of 2.0 μM (S/N = 3) under optimized conditions. The apparent Michaelis–Menten constant (K_M^{app}) was evaluated to be 1.3 mM. The sensor exhibited high sensitivity, good accuracy and an acceptable stability.

1. Introduction

Highly sensitive and selective determination of H_2O_2 is of great importance in food, clinical, biological, environmental and many other fields. Many analytical methods have been developed for this purpose, such as titrimetry, photometry and electrochemistry. Among these methods, amperometric enzyme-based biosensors have received considerable attention due to its convenience, high sensitivity and selectivity [1,2]. However, a significant challenge to development of sensitive and stable sensors comes from the effective immobilization of enzyme to solid electrode surface [3]. Up to now, many materials have been used to immobilize enzyme on the surface of electrodes, such as quantum dots [4], polymers [5,6], mesoporous materials [7] and nanomaterials [8–10]. Among these materials, nanomaterials, especially functionalized nanocomposites have attracted great research interest in biosensor because of their versatility of the physical and chemical properties and other properties [11]. For example, SiO_2 functionalized by 3-aminopropyltrimethoxysilane was used in the glucose biosensor [12]. Zhang et al. immobilized tyrosinase in inorganic–organic hybrid titanium-oxo-polymers nanocomposite [13]. Ma et al. fabricated a polyaniline–TiO_2 composite film with in situ polymerization approach to detect trimethylamine at room temperature [14]. However, the conductivity is not very good because they are semiconductor nanocomposites, which resulted in the low sensitivity and the low accuracy in some degree, thereby they are limited in the biosensing application. Recently, more and more conducting metal nanoparticles modified by other materials were synthesized and applied widely in diverse areas. Tan et al. reported thiosalicylic acid-functionalized Ag nanoparticles which was synthesized in one-phase system [15]. Liu and Jiang used Nafion and PDDA–Pt nanoparticles synthesized by the alcoholic reduction of the Pt ions in ethanol/water system to construct polymer electrolyte fuel cells [16]. Wohltjen and Snow first reported the use of an octanethiol-coated Au nanoparticle material as a thin film on a chemiresistor device [17]. Hang and Chang proposed a novel colorimetric method for mercury (II) in aqueous solutions using mercaptopropionic acid-modified Au nanoparticles in presence of 2,6-pyridinedicarboxylic acid as a more stable complex compound with heavy metal ions than other metal ions [18]. To our best knowledge, although many applications of conducting metal nanoparticles modified by other materials have been reported, very few studies have been carried out for construction of hydrogen peroxide biosensor by taking advantage of the merits of composite materials which combine together the different properties of components and lead the way to a new, tunable behavior [19]. So, in this paper, we fabricated a hydrogen peroxide biosensor formed with DNA–Ag and PDDA–Au to entrap horseradish peroxidase (HRP).

* Corresponding author. Tel.: +86 23 68252277; fax: +86 23 68252277.
E-mail addresses: ping319@163.com (L. Ma), yuanruo@swu.edu.cn (R. Yuan).

1381-1177/$ – see front matter.
doi:10.1016/j.molcatb.2008.05.007

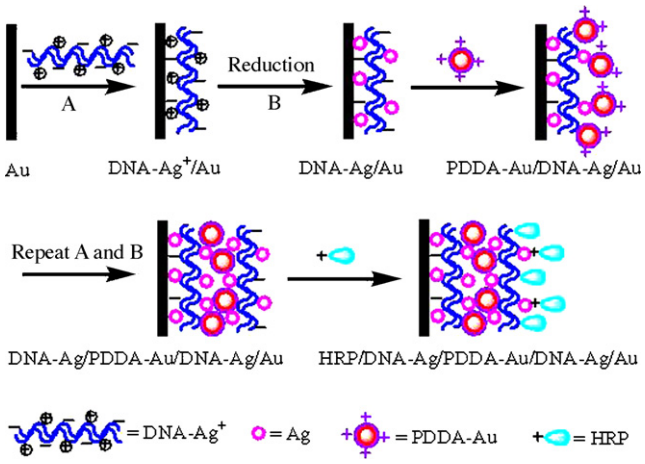

Scheme 1. Illustration of the preparation process of modified electrode.

First, we electrochemically reduced the DNA–Ag^+ complex to obtain negatively charged immobilization matrix (DNA–Ag) to immobilize PDDA–Au. Here, immobilization of PDDA–Au was attributed to the two forces. The one is electrostatic force between positively charged PDDA–Au and the negatively charged DNA. The other is the adsorption of the nano-Ag to the PDDA–Au. Then, the second layer of DNA–Ag was assembled onto the modified electrode based on the electrostatic force and excellent film-forming ability of DNA. Finally, the positively charged HRP was adsorbed tightly onto the DNA–Ag layer just as the adsorption of PDDA–Au to obtain hydrogen peroxide biosensor without losing their biological activity (see Scheme 1).

This strategy has following advantages. First, Au and Ag nanoparticles not only possess larger specific surface area, good biocompatibility, but also possess good conductivity. They can make possible conducting channels to facilitate charge transfer between the prosthetic groups and the electrode surface [20]. Secondly, PDDA can act as the reducing and stabilizing agents to fabricate the PDDA-protected Au nanoparticles simultaneously [21]. Furthermore, PDDA is a positively charged ionic polymer, and the PDDA-protected Au nanoparticles can be effectively self-assembled onto the negatively charged DNA–Ag membrane by electrostatic interaction. DNA, a robust negatively charged biopolymer with excellent film-forming and adhesion ability, biocompatibility and the efficient electroconductivity [22], is widely recognized as an ideal candidate for enzyme immobilization. Finally, compared with the other methods, our proposed strategy in this paper is not necessary to introduce any other noxious material or energy to the system, so it is very good to avoid the contamination and deactivation of the enzyme [20] and obtain a hydrogen peroxide biosensor which showed high sensitivity, an acceptable stability and good repeatability.

2. Experimental

2.1. Reagents and apparatus

HRP, gold chloride ($HAuCl_4$), poly(diallyldimethylammonium chloride) (PDDA, MW 200,000–350,000) and double-stranded calf thymus DNA were all obtained from Sigma Chemical Co. Silver nitrate ($AgNO_3$, AR) and potassium nitrate (KNO_3, AR) were purchased from Beijing Chemical Co. (China). Hydrogen peroxide (H_2O_2, 30%, w/v solution) was purchased from Chemical Reagent Co. (Chongqing, China). The concentration of the more diluted hydrogen peroxide solutions prepared from 30% hydrogen peroxide was determined by titration with potassium permanganate. All other chemicals employed were of analytical grade and were used without further purification. All solutions were made up with doubly distilled water.

Electrochemical measurements were performed on CHI660A electrochemical workstation (CH Instruments, Chenhua Co., Shanghai, China). A conventional three-electrode system was employed with a modified Au disk electrode (φ = 4.0 mm) as a working electrode, a platinum wire as an auxiliary electrode, and a saturated calomel electrode (SCE) as a reference electrode. All the potentials given in this paper were referred to the SCE. The size of PDDA–Au was estimated from transmission electron microscopy (TEM, TECNAI 10, Philips Fei Co., Holland). UV–vis absorption spectra were recorded in the range of 250–700 nm using a Lambda 17 UV–vis 8500 spectrometer (PE Co., USA) with a quartz cell (path length 1 cm) at room temperature. The morphologies of the bare Au and the substrate modified with different materials were investigated with atomic force microscope (AFM, Vecco, USA).

2.2. Preparation of PDDA–Au nanoparticles

PDDA–Au nanoparticles were synthesized according to Ref. [21] with a little change. Briefly, 250 μL PDDA solution of certain concentration, 40 mL water, 200 μL 0.5 M NaOH and 100 μL $HAuCl_4$ (1%) were added into a beaker. After thoroughly mixed for a few minute, the mixed solution continued heating until the color of the solution changed to red and no further color change occurred. The UV–vis spectrum and TEM were used to confirm and characterize the production. Fig. 1 shows UV–vis spectra of PDDA solution (curve a) and PDDA–Au solution (curve b). When the solution just only contained PDDA, no obvious absorption peak can be observed. But when the solution contained the production, a maximum adsorption in UV–vis spectrum was observed at 524 nm, which is a typical plasmon absorbance of spherical Au nanoparticles [21–23]. It is proved that PDDA–Au nanoparticles have been successfully synthesized. In order to further confirm and characterize the size and size distribution of PDDA–Au nanoparticles, Fig. 2 shows typical TEM image of the PDDA–Au nanoparticles. As shown in Fig. 2, all of the PDDA–Au nanoparticles are almost spherical, evenly distributed without obvious aggregation and the average diameter is about 15 nm. This is ascribed to the surrounding PDDA polymers, which could limit particle aggregation and thus yielded uniform, isolated, small particles.

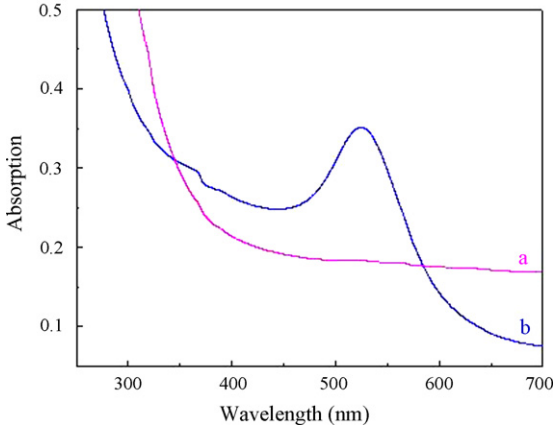

Fig. 1. UV–vis absorption spectrum of PDDA solution (a) and PDDA–Au solution (b).

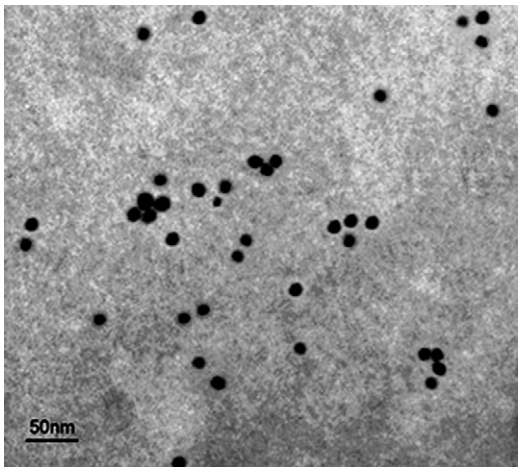

Fig. 2. Typical TEM image of the PDDA–Au.

2.3. Preparation of hydrogen peroxide biosensor

The bare Au disk electrode was polished successively with 0.3 and 0.05 μm alumina slurry, and ultrasonically cleaned in ethanol and double-distilled water before modification. First, the solution of DNA–Ag^+ was produced by adding a silver nitrate solution to a 1.0 mg/mL DNA solution, where the final concentration of Ag was 4 mM. Then, 15 μL DNA–Ag^+ solution were dropped onto the cleaned Au electrode surface. After that, the electrode was dried in air, and was reduced electrochemically to yield DNA–Ag nanohybrids under a constant potential of −0.4 V in 0.1 M KNO_3 solution for 1000 s [11]. Following that, it was soaked in PDDA–Au solution for 6 h. Subsequently, the second layer of the DNA–Ag was assembled onto the resulting electrode as the above method. At last, the electrode was immersed in HRP solution (5 mg/mL, 0.1 M pH 6.5 PBS) for 12 h to obtain the hydrogen peroxide biosensor. For comparison, the electrode without Au, Ag nanoparticles and HRP were prepared similarly. All the resulting electrodes were stored at 4 °C when not in use.

3. Results and discussion

3.1. AFM characterization

AFM technique was employed to confirm the self-assembled process of the biosensor construction. Typical AFM images of the bare Au and the Au substrate modified with different materials were shown in Fig. 3. Bare Au substrate displayed an even surface and root mean square roughness (R_{rms}) was 0.824 nm (Fig. 3a). However, the surface morphology of the DNA–Ag/Au electrode presented an amount of homogeneous, dense and spherical Ag nanoparticles, and the R_{rms} increased to 10.473 nm (Fig. 3b), which confirmed Ag^+ were effectively electrochemically

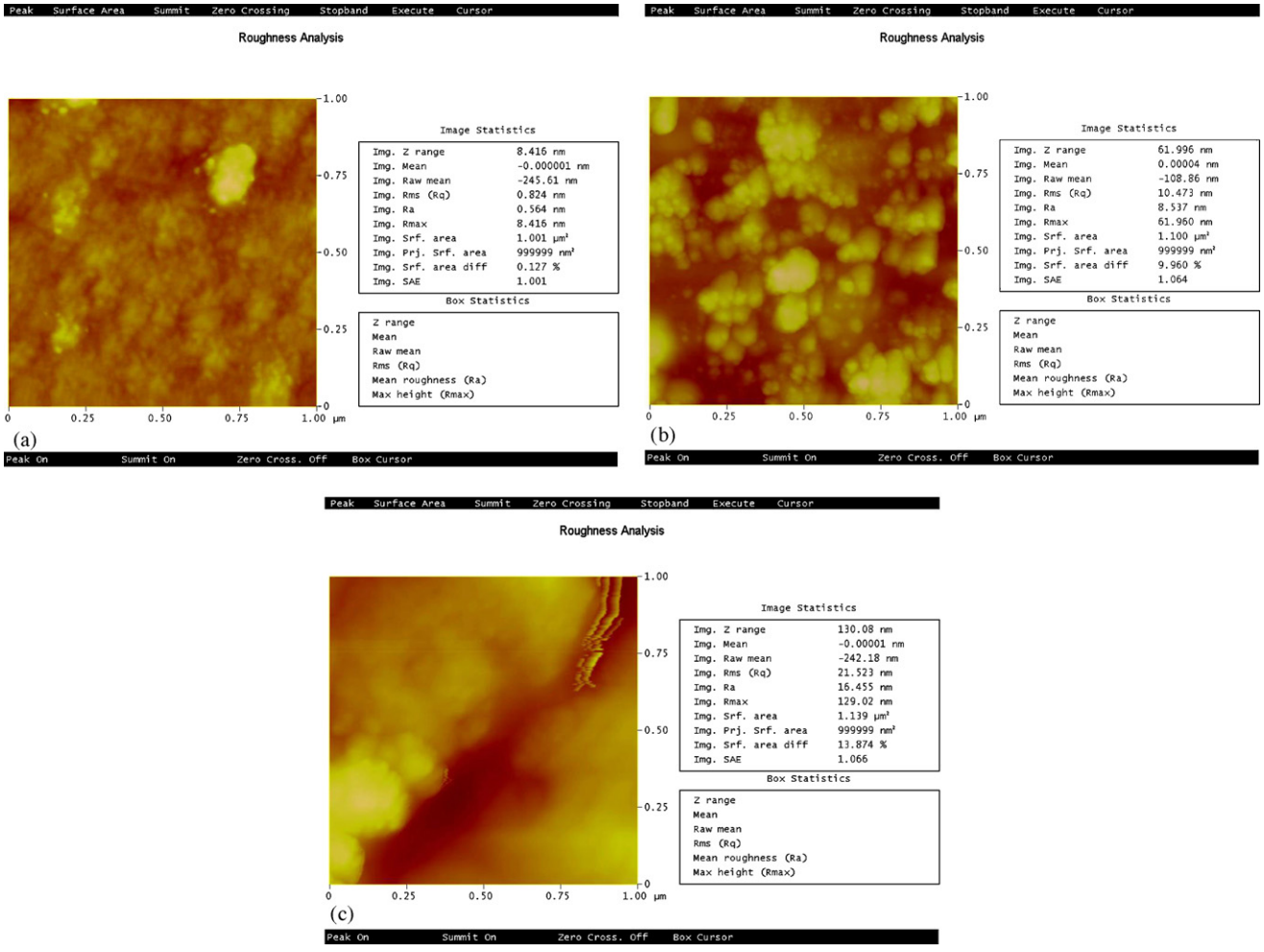

Fig. 3. AFM images of bare Au substrate (a), DNA–Ag (b) and HRP/DNA–Ag/PDDA–Au/DNA–Ag (c) on Au surfaces.

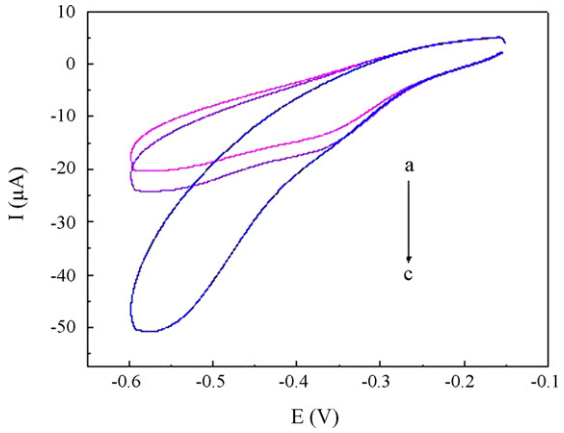

Fig. 4. CVs of biosensor at a scan rate of 50 mV/s in 0.1 M PBS (pH 6.0) without H_2O_2 (a), with 0.07 mM H_2O_2 (b) and 0.7 mM H_2O_2 (c).

reduced to Ag nanoparticles. After HRP was immobilized onto the DNA–Ag/PDDA–Au/DNA–Ag/Au electrode, its surface was covered with a layer of compact and well organized assembly materials and the R_{rms} changed to 21.523 nm (Fig. 3c), which are significantly different from that of Fig. 3b, indicating that HRP was successfully adsorbed on the surface of DNA–Ag/PDDA–Au/DNA–Ag/Au electrode.

3.2. Electrochemical behavior of hydrogen peroxide biosensor

The electrocatalytic behavior of the biosensor towards H_2O_2 was investigated by cyclic voltammetry. Fig. 4 shows the bioelectrocatalytic behavior of the hydrogen peroxide biosensor in 0.1 M PBS of pH 6.0. In the absence of H_2O_2, no obvious current was found (Fig. 4a), but with the addition of H_2O_2, the catalytic current increased evidently (Fig. 4b and c). It demonstrated that HRP immobilized on DNA–Ag nanohybrids and PDDA–Au nanoparticles shows good catalytic activity toward H_2O_2. Typical cyclic voltammograms of the biosensor in 0.1 M PBS (pH 6.0) at scan rates ranging from 30 to 250 mV/s were shown in Fig. 5. There was a linear relation between the reduction peak currents and the square root of scan rate ($v^{1/2}$), as shown in the inset of Fig. 5, indicating diffusion control process.

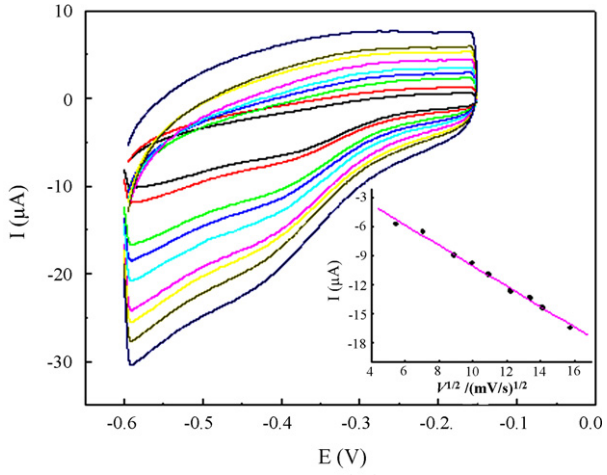

Fig. 5. CVs of the biosensor at different scan rates (from inner to outer): 30, 50, 80, 100, 120, 150, 180, 200 and 250 mV/s in 0.1 M PBS (pH 6.0). Inset: plots of reduction peak currents versus $v^{1/2}$.

3.3. Optimum conditions of the biosensor

In order to obtain an efficient biosensor for H_2O_2, the influence of pH and applied potential on the response of the modified electrode were investigated. The effect of pH on the modified electrode was investigated in the pH range 4.5–8.5 in the presence of 0.07 mM H_2O_2. It can be seen that the response increased clearly from pH 4.5 to pH 6.0, and reached the maximum at pH 6.0, then the further increase of buffer pH led to decrease of the response (Fig. 6A), indicating that the catalytic response were controlled by the enzymatic activity. Decrease in the response at high pH was possibly due to the decrease of enzymatic activity. So the pH 6.0 PBS solution was chosen as optimal PBS solution. Applied potential was also an important factor affecting the amperometric response of the biosensor. Fig. 6B shows the dependence of the chronoamperometric current response to constant concentration (0.07 mM) H_2O_2 on the applied potential. Although amperometric current increased gradually when the applied potential shifted from 0 to −0.5 V, an applied potential of −0.35 V was selected for the amperometric determination of H_2O_2. Because we not only could obtain sufficient current responses but also could minimize the risk for interfering reactions of other electroactive species in the solution at −0.35 V.

We compared the chronoamperometry response of differently modified electrodes in the PBS (pH 6.0) at applied potential of −0.35 V, as shown in Fig. 7. The proposed biosensor was HRP/DNA–Ag/PDDA–Au/DNA–Ag/Au electrode (Fig. 7d), its response current increased sharply from about 10 to 140 μA with successive injections of 0.35 mM H_2O_2. Compared with it, the HRP/DNA/PDDA–Au/DNA/Au electrode (Fig. 7a) and HRP/DNA–Ag/PDDA/DNA–Ag/Au electrode (Fig. 7c) exhibited less sensitive amperometric responses to H_2O_2 as the lack of Au or Ag nanoparticles. This phenomenon is consistent with the fact that the hetero-metal nanoparticles often present a better catalytic characteristic compared to the single metal [24]. Without the HRP, the DNA–Ag/PDDA–Au/DNA–Ag/Au electrode (Fig. 7b) also appeared certain electrochemical catalysis response to H_2O_2, which can be attributed to the inherent catalysis of Au or Ag nanoparticles. Compared with Fig. 7b, Fig. 7d exhibited more sensitive response to H_2O_2. From these results, we confirmed that the immobilization of the HRP showed high biological activity to H_2O_2, and the catalytic current was mainly due to the direct electron transfer from the HRP molecules to the bare Au electrode. However, these nanoparticles distributed on the surface of Au electrode mainly acted as the carrier to immobilize the HRP molecules and the tiny conduction centers to facilitate the transfer of electrons [20,25].

3.4. Chronoamperometric response and calibration curve

Fig. 8 displays typical current–time curves of the biosensor to reduction of H_2O_2 under optimized conditions. The response current increases markedly with increasing concentration of H_2O_2. There is an excellent linear relation of the current with concentration of H_2O_2 from 7.0 μM to 7.8 mM, as shown in the lower inset of Fig. 8. The linear regression equation is $i\,(\mu A) = -7.7 - 16.6[H_2O_2]$ (mM) with a correlation coefficient of 0.999 ($n = 23$). From the slope of calibration curve, the detection limit of 2.0 μM is estimated at signal-to-noise ratio of 3, and the sensitivity of the biosensor is 0.11 A M^{-1} cm^{-2}. This value is higher than that reported in the literatures, e.g., 0.013 A M^{-1} cm^{-2} at a chitosan-entrapped carbon paste electrode with HRP adsorption [26], 0.0085 A M^{-1} cm^{-2} based on immobilization of HRP in MB-Bir [27], 0.0014 A M^{-1} cm^{-2} using Chi-AOB composite film as immobilization of HRP [28]. In addition, the proposed biosensor reached 95% of steady-state current within 15 s. All these merits are mainly attributed to the presence of DNA, Au and Ag nanoparticles, which improved the conductivity

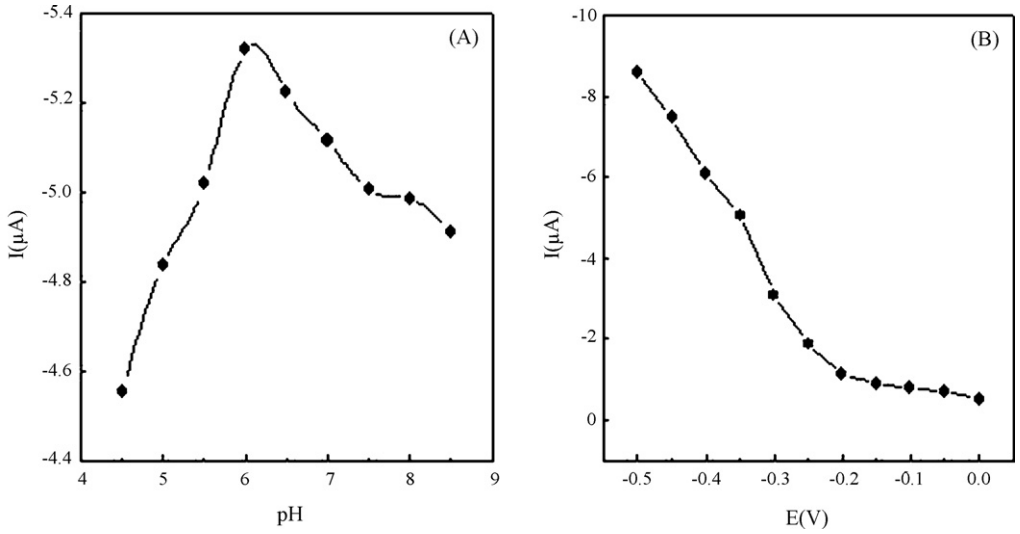

Fig. 6. Dependence of the current response of biosensor to 0.07 mM H_2O_2 on the pH of buffer solutions at an applied potential of −0.35 V (A) and on the applied potential in 0.1 M PBS (pH 6.0) (B).

of the composite film and made conducting channels between the prosthetic groups and the electrode surface, and reduced the effective electron transfer distance to facilitate charge transfer between electrode and HRP. Consequently, the signal of response current has been magnified and the sensitivity has been enhanced.

The apparent Michaelis–Menten constant (K_M^{app}) is an indication of the enzyme–substrate kinetics. According to the Lineweaver–Burk equation [29]:

$$\frac{1}{I_{ss}} = \frac{1}{I_{max}} + \frac{K_M^{app}}{I_{max}C}$$

where I_{SS} is the steady-state current after the addition of substrate, I_{max} is the maximum current under saturated substrate condition and C is the bulk concentrate of the substrate. The value of the apparent Michaelis–Menten constant (K_M^{app}) can be calculated from the slope (K_M^{app}/I_{max}) and the intercept ($1/I_{max}$) for the plot of the reciprocals of the steady-state current (I_{SS}) versus H_2O_2 concentration (C). Thus the K_M^{app} value for the modified electrode was calculated to be 1.3 mM. This K_M^{app} value is smaller than that obtained for HRP incorporated in Au nanoparticles and chitosan composite film (K_M^{app} = 4.51 mM) [30], in poly(thionine) film (K_M^{app} = 28 mM) [31] and nano-Ag/DNA membrane (K_M^{app} = 1.62 mM) [32]. This result suggests that HRP immobilized in DNA–Ag/PDDA–Au/DNA–Ag film retains its bioactivity and has a high biological affinity to H_2O_2.

3.5. Repeatability and stability of the hydrogen peroxide biosensor

The relative standard deviation (R.S.D.) of the biosensor response to 0.35 mM H_2O_2 was 3.9% for 8 successive measurements, showing the proposed biosensor possesses a good reproducibility.

The storage stability of the proposed biosensor was also studied. When not in use, the biosensor was stored dry at 4 °C and measured at intervals of a week, and it lost only 5.2% of the initial response after 2 weeks and maintained more than about 78.4% of the initial values after storage for 1 month. These values are lower than that obtained for HRP immobilized in the poly-thionine nanowire and nano-Au composite nanomaterial [33], but higher than that

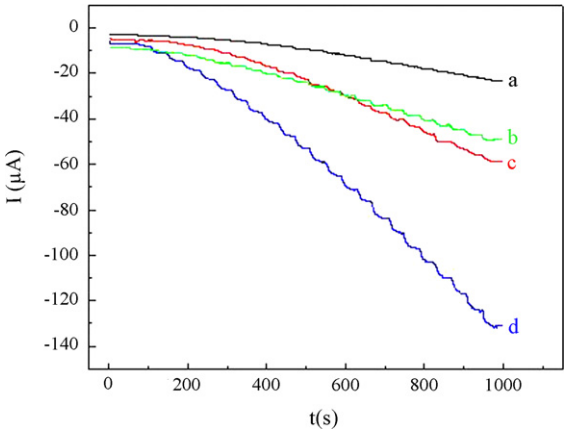

Fig. 7. The chronoamperometry response at applied potential of −0.35 V with successive injection of 0.35 mM H_2O_2 into a stirred solution of 0.1 M PBS (pH 6.0) for HRP/DNA/PDDA–Au/DNA (a), DNA–Ag/PDDA–Au/DNA–Ag (b), HRP/DNA–Ag/PDDA/DNA–Ag (c) and HRP/DNA–Ag/PDDA–Au/DNA–Ag-modified Au electrode (d), respectively.

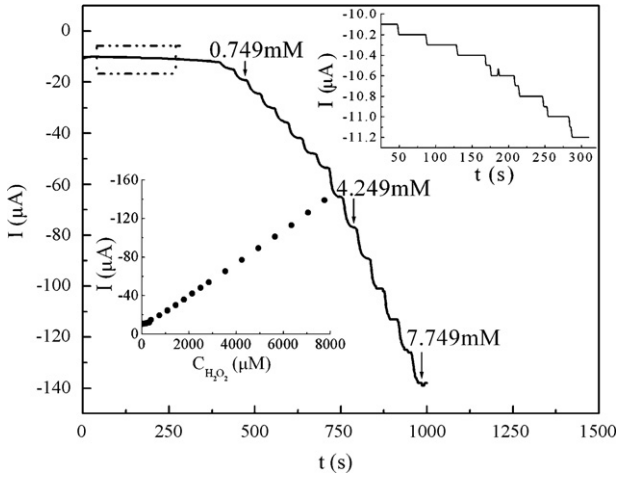

Fig. 8. Typical current–time response of the biosensor on successive injection of different concentration of H_2O_2 into a stirred solution of 0.1 M PBS (pH 6.0) at an applied potential of −0.35 V in the time intervals of 40 s. Lower inset: linear calibration curves; upper inset: amplified response curve.

Table 1
Possible interferences tested with the hydrogen peroxide biosensor

Possible interferences	Current ratio
L-Cysteine	0.96
L-Tyrosine	0.97
Ethanol	0.99
Acetic acid	1.01
Glucose	1.02
Ascorbic acid	1.05

in methylene blue-incorporated double-stranded DNA–polyamine complex membrane [34]. So, the proposed biosensor shows an acceptable stability, which can be attributed to the two aspects. On the one hand, using DNA–Ag nanohybrids as matrix to entrap HRP provided biocompatible microenvironment for retaining the native activity of HRP. On the other hand, introducing the self-assembly technique to immobilize HRP was a mildly immobilization process which did not involve any poisonous material or the chemical modification of the enzyme molecule.

3.6. Selectivity of the hydrogen peroxide biosensor

Selectivity is also important in practical use of the biosensors. In order to investigate the effect of some possible interfering substances on the biosensor, 6 interfering substances were used for measurement in our experiments. The results are listed in Table 1. The current ratios were calculated by reading the current of the biosensor in the assay solution containing 0.35 mM interfering substance and 0.35 mM H_2O_2 and comparing it with the current from the biosensor in the same assay solution containing only 0.35 mM H_2O_2. According to the results of the current ratio, we can find that the 6 tested substances did not interfere significantly with the resulting biosensor, which was mainly attributed to the low working potential of −0.35 V used in the determination of H_2O_2.

4. Conclusions

In this work, a novel and simple hydrogen peroxide biosensor was successfully fabricated by immobilizing the model enzyme, HRP, on the DNA–Ag/PDDA–Au/DNA–Ag film formed by electrochemical reduction method and self-assembly technique. Because these composite combined the advantages of inorganic metal species (Au and Ag) and organic polymer (PDDA and DNA), the biosensor exhibited satisfactory sensitivity and accuracy for the fast detection of H_2O_2. In addition, these composite materials can also conveniently extend to the immobilization of other biomolecules.

Acknowledgments

Financial support of this work was provided by the National Natural Science Foundation of China (20675064), the Natural Science Foundation of Chongqing City (CSTC-2004BB4149, 2005BB4100), China and High Technology Project Foundation of Southwest University (XSGX 02), China.

References

[1] T.T. Gu, Y. Hasebe, Biosens. Bioelectron. 21 (2006) 2121.
[2] S.H. Chen, R. Yuan, Y.Q. Chai, L.Y. Zhang, N. Wang, X.L. Li, Biosens. Bioelectron. 22 (2007) 1268.
[3] D. Du, J.W. Ding, J. Cai, A.D. Zhang, Colloids Surf. B 58 (2007) 145.
[4] Q. Liu, X.B. Lu, J. Li, X. Yao, J.H. Li, Biosens. Bioelectron. 22 (2007) 3203.
[5] Y.X. Sun, J.T. Zhang, S.W. Huang, S.F. Wang, Sens. Actuators B 124 (2007) 494.
[6] J. Li, X.Q. Lin, Biosens. Bioelectron. 22 (2007) 2898.
[7] Q. Xu, J.J. Zhu, X.Y. Hu, Anal. Chim. Acta 597 (2007) 151.
[8] L. Wang, E.K. Wang, Electrochem. Commun. 6 (2004) 225.
[9] Y.H. Yang, H.F. Yang, M.H. Yang, Y.L. Liu, G.L. Shen, R.Q. Yu, Anal. Chim. Acta 525 (2004) 213.
[10] J.D. Zhang, M.L. Feng, H. Tachikawa, Biosens. Bioelectron. 22 (2007) 3036.
[11] L. Shang, Y.L. Wang, L.J. Huang, S.J. Dong, Langmuir 23 (2007) 7738.
[12] Y.Y. Sun, F. Yan, W.S. Yang, C.Q. Sun, Biomaterials 27 (2006) 4042.
[13] T. Zhang, B.Z. Tian, J.L. Kong, P.Y. Yang, B.H. Liu, Anal. Chim. Acta 489 (2003) 199.
[14] X.F. Ma, M. Wang, G. Li, H.Z. Chen, R. Bai, Mater. Chem. Phys. 98 (2006) 241.
[15] Y.W. Tan, Y. Wang, L. Jiang, D.B. Zhu, J. Colloid Interf. Sci. 249 (2002) 336.
[16] Z.C. Liu, S.P. Jiang, J. Power Sources 159 (2006) 55.
[17] H. Wohltjen, A.W. Snow, Anal. Chem. 70 (1998) 2856.
[18] C.C. Hang, H.T. Chang, Chem. Commun. (2007) 1215.
[19] E. Pintér, R. Patakfalvi, T. Fülei, Z. Gingl, I. Dékány, C. Visy, J. Phys. Chem. B 109 (2005) 17474.
[20] W.W. Yang, J.X. Wang, S. Zhao, Y.Y. Sun, C.Q. Sun, Electrochem. Commun. 8 (2006) 665.
[21] H.J. Chen, Y.L. Wang, Y.Z. Wang, S.J. Dong, E.K. Wang, Polymer 47 (2006) 763.
[22] X.Q. Lin, G.F. Kang, L.P. Lu, Bioelectrochemistry 70 (2007) 235.
[23] J.W. Kang, X.N. Li, G.F. Wu, Z.H. Wang, X.Q. Lu, Anal. Biochem. 364 (2007) 165.
[24] R.D. Adams, J. Organomet. Chem. 600 (2000) 1.
[25] S.Y. Xu, G.L. Tu, B. Peng, X.Z. Han, Anal. Chim. Acta 570 (2006) 151.
[26] C.X. Lei, S.Q. Hu, G.L. Shen, R.Q. Yu, Talanta 59 (2003) 981.
[27] X.S. Yang, X. Chen, X. Zhang, W.S. Yang, D.G. Evans, Sens. Actuators B 129 (2008) 784.
[28] X.B. Lu, Z.H. Wen, J.H. Li, Biomaterials 27 (2006) 5740.
[29] R.A. Kamin, G.S. Wilson, Anal. Chem. 52 (1980) 1198.
[30] T. Tangkuaram, C. Ponchio, T. Kangkasomboon, P. Katikawong, W. Veerasai, Biosens. Bioelectron. 22 (2007) 2071.
[31] Y. Xiao, H.X. Ju, H.Y. Chen, Anal. Chim. Acta 391 (1999) 299.
[32] F.C. Wang, R. Yuan, Y.Q. Chai, D.P. Tang, Anal. Bioanal. Chem. 387 (2007) 709.
[33] A.W. Shi, F.L. Qu, M.H. Yang, G.L. Shen, R.Q. Yu, Sens. Actuators B 129 (2008) 779.
[34] T.T. Gu, Y. Hasebe, Anal. Chim. Acta 525 (2004) 191.